11-2019

Flexibility of Remediation Methods for Winding Open Circuit Faults in a Multiphase PM Machine Considering Iron Losses Minimization

Fan Wu
Marquette University, fan.wu@marquette.edu

Ayman M. EL-Refaie
Marquette University, ayman.el-refaie@marquette.edu

2019 IEEE Energy Conversion Congress and Exposition (ECCE), (September 29, 2019 – October 03, 2019): 3889-3896. DOI.

Flexibility of Remediation Methods for Winding Open Circuit Faults in a Multiphase PM Machine Considering Iron Losses Minimization

Fan Wu
Department of Electrical and Computer Engineering, Marquette University, Milwaukee, WI
Ayman M. EL-Refaie
Department of Electrical and Computer Engineering, Marquette University, Milwaukee, WI

Abstract:

The flexibility of post-fault control in multiphase machine systems stems from their multiple degrees of freedom. A post-fault loss-minimization method is proposed and investigated in this paper, in which

both the machine copper and iron losses are considered during the derivation of post-fault remediation methods. Therefore, machine efficiency during post-fault operation can be further improved compared to the conventional stator-ohmic-loss-minimization approach. In addition, the combination of three key factors/constraints that can influence the post-fault control strategy of a six-phase permanent magnet (PM) machine has been investigated. By comparing four selected remediation methods based on three constraints, the pros and cons of those methods as well as the influence of the constraints are discussed.

SECTION I. Introduction

The fast growth of multiphase permanent-magnet (PM) machines and drives has been observed in various applications like ship propulsion, electric/hybrid-electric vehicles, electrified aircraft, etc. [1]. The key advantages of multiphase machine systems include the following,

- *Low-voltage high-power design*: by having higher number of phases, the power rating for each individual phase gradually goes down. This addresses the voltage limit issues in many high-power systems like ship propulsion and offshore wind generators;
- *Fault-tolerant capability*: more design degrees of freedom enable uninterrupted operation following faults and flexible post-fault control strategies. This is of paramount significance for safety-critical applications like aerospace;
- *Flexibility of system design and control*: This includes, for example, integrated sensorless control, integrated onboard battery chargers, cascaded DC bus to unitize elevated voltage, etc.

A variety of post-fault remediation methods for winding open faults have been investigated. Although in many cases, those approaches are proposed to deal with open circuit faults, they can be easily extended for winding short circuit faults as well.

Two of the well-known post-fault control strategies are based on **(i)** constant torque-producing magnetomotive force (MMF) [2]; **(ii)** instantaneous power balance theory, in which the electromagnetic power becomes the target of post-fault control [3]. In terms of the degrees of freedom in current regulation of multiphase machines, many of the control factors have been discussed in conjunction with those approaches. These include shapes of winding back electromotive force (EMF) (quasi-sinusoidal or trapezoid waveform), pattern of winding connection/drive topologies (with or without neutral point constraint), fault location, stator ohmic loss minimization, torque ripple minimization, etc. By taking into account one or more of those factors, the optimum remediation methods can be derived [4]. However, a comprehensive discussion of the combination of different key factors is still missing in literature. Also, the comparison between different remediation methods has not been explored yet. In addition, the loss minimization method used in existing post-fault control strategies only considers stator copper losses. However, the machine efficiency is mainly determined by iron and copper losses (other losses are not associated with winding excitations). Also, whether constant torque-producing MMF or instantaneous power balance theory ignore the fact that unbalanced current amplitude changes the maximum thermal capability required and the required higher current rating of power electronics in some cases.

Other than the fundamental component, harmonic MMF components have been taken into account as well. In case of winding one-phase and two-phase open-circuit faults, the third harmonic injection has been used to eliminate the second and fourth harmonics of electromagnetic torque in a five-phase fractional-slot concentrated-winding (FSCW) PM machine [5]. The importance of considering the third harmonic back EMF has been verified for winding short-circuit current prediction, torque pulsation and post-fault control strategy as well [6].

The objective of this paper is to further explore the flexibility of post-fault operation under winding open-circuit fault and compare machine performance under different remediation methods. A six-phase FSCW-PM machine has been used as an example to examine and compare the investigated remediation methods. The paper is arranged as follows: Section II covers the stator iron loss calculation in case of open circuit faults and a loss minimization approach considering both machine copper and iron losses; Section III discusses the key constraints and factors for post-fault remediation method as well as four selected approaches; Conclusions are drawn in Section IV.

SECTION II. Modeling of Iron Loss Under Faulty Modes

A. Modeling of iron losses in case of open circuit fault

Prediction of machine iron losses has been demonstrated for three-phase AC machines during normal operation [7], [8]. This section will extend the method for predicting iron losses under faulty conditions. A multiphase single-layer FSCW-SPM machine is used for this analysis, which features negligibly small mutual coupling between phase windings. Iron losses can be an issue for FSCW-SPM machines, since the number of poles is generally high which results in high electrical frequencies.

Assume that Phase F is open-circuited, the target of any post-fault control strategies is to achieve constant d-, q- components, so that the torque ripple can be minimized. d- and q-axis current can be obtained by Park and Clark transformations from "*abcde*" reference frame to " $dqz_1z_2z_3$" reference frame,

$$I_{dqz_1z_2z_3} = T_{Clark}T_{Park}I_{abcde}$$

(1)

where $I_{abcde} = [i_a;\ i_b;\ i_c;\ i_d;\ i_e]$ denotes currents in the remaining five phases; $I_{dqz_1z_2z_3} = [i_d;\ i_q;\ i_{z1};\ i_{z2};\ i_{z3}]$ represents currents in " $dqz_1z_2z_3$" reference frame; Park and Clark transformation matrixes for single-phase open fault are given by,

$$T_{Park} = \begin{bmatrix} 0.5774 & 0.5 & -0.2887 & -0.5 & -0.2887 \\ 0 & 0.3536 & 0.6124 & 0.3536 & -0.6124 \\ -0.4177 & 0.5706 & -0.5706 & 0.4177 & 0 \\ -0.5196 & 0.4177 & 0.3804 & -0.5706 & 0.2921 \\ 0.4714 & 0.3536 & 0.2673 & 0.3536 & 0.6755 \end{bmatrix}$$

(2)

(based on power invariance method [9])

$$T_{Clark} = \begin{bmatrix} \cos\theta & \sin\theta & 0 & 0 & 0 \\ -\sin\theta & \cos\theta & 0 & 0 & 0 \\ 0 & 0 & \cos 5\theta & \sin 5\theta & 0 \\ 0 & 0 & -\sin 5\theta & \cos 5\theta & 0 \\ 0 & 0 & 0 & 0 & 1 \end{bmatrix}$$

(3)

where θ is electric angle of rotor.

Since the "$z_1 z_2 z_3$" plane presents non-torque-producing components, "$z_1 z_2 z_3$" components are usually minimized during post-fault control. In this regard, iron losses are mainly produced by d- and q-axis components.

Flux linkage and flux are given by,

$$\begin{cases} \psi_d = L_d i_d + \psi_{pm} \\ \psi_q = L_q i_q \end{cases}$$

$$\begin{cases} \Phi_d = \dfrac{\sqrt{2}\psi_d}{\sqrt{5} N_s k_{dp1}} \\ \Phi_q = \dfrac{\sqrt{2}\psi_q}{\sqrt{5} N_s k_{dp1}} \end{cases}$$

(4)(5)

where $\psi_{d,q}$ are d- and q-axis flux linkages; ψ_{pm} is PM flux linkage; $L_{d,q}$ are d- and q-axis inductances; N_S denotes number of series turns per phase; k_{dq1} is the winding factor for fundamental (synchronous) MMF component.

Amplitude of flux density in stator teeth and stator yoke can be obtained by,

$$\begin{cases} B_{td,q} = \dfrac{2p\Phi_{d,q}}{\alpha_l S_t Q} \\ B_{sd,q} = \dfrac{\Phi_{d,q}}{2S_y} \end{cases}$$

(6)

where p is number of pole pairs; $\Phi_{d,q}$ are d- and q- axis flux; $S_t,\ S_y$ are cross-section area of stator teeth and stator yoke, respectively; Q denotes number of stator slots; $\alpha_i = W_t/(W_t + W_s)$ where W_t and W_s are tooth and slot width, respectively; $Btd, q,\ B_{sd},\ q$, are the amplitude of flux density in the stator teeth and yoke, respectively.

The decoupled transformation used for symmetrical six-phase machine can be found in [10]. It can be extended to asymmetrical six-phase machine under open-circuit fault (two 3-phase sets shifted by 30 degree), which is discussed in this paper. It should be noted that cross-coupling is ignored. By using the Bertotti iron loss formula [11], the iron losses, which include eddy current losses, hysteresis losses and excess loss, can be predicted as follows,

$$\begin{cases} P_{Fet} = \left\{ \left[k_h f + \dfrac{\pi^2 \sigma k_d^2}{6} f^2 \right] \left(B_{td}^2 + B_{tq}^2 \right) + k_e f^{1.5} \left(B_{td}^{1.5} + B_{tq}^{1.5} \right) \right\} V_t \\ P_{Fey} = \left\{ \left[k_h f + \dfrac{\pi^2 \sigma k_d^2}{6} f^2 \right] \left(B_{sd}^2 + B_{sq}^2 \right) + k_e f^{1.5} \left(B_{sd}^{1.5} + B_{sq}^{1.5} \right) \right\} V_y \end{cases}$$

$$\begin{cases} V_t = Q h_t S_t \\ V_y = \pi \left(D_{so} - h_y \right) S_y \end{cases}$$

(7)(8)

where k_h, k_e, k_d are hysteresis loss coefficient, excess loss coefficient, and lamination thickness, respectively; σ is the conductivity of the lamination steel sheet; $f = np/60$ is electrical frequency; V_t, V_y are the volume of lamination steel for stator teeth and stator yoke, respectively; h_t is the height of stator teeth; D_{so} is stator outer diameter.

Therefore, the total stator iron losses are:

$$P_{Fe} = P_{Fet} + P_{Fey}$$

(9)

where P_{Fet} and P_{Fey} represent iron losses in stator teeth and yoke respectively.

B. Implementation of iron loss calculation

The key dimensions and parameters of the machine design used for iron loss estimation are summarized in Table I while a sketch of the machine cross section is shown in Fig. 1.

TABLE I Summary of Key Dimensions and Parameters of the Six-Phase Machine Design

Dimensions/Parameters	**Value**
Spinning speed [r/min]	450 (corner); 1200 (max.)
Stack length [mm]	101
Series turns per phase	144
S_t (section area of stator teeth) [mm^2]	1961.7
S_y (section area of stator yoke) [mm^2]	1211.9
W_t (width of stator teeth) [m]	18
W_s (width of stator slot) [m]	14.4
h_t (height of stator teeth) [mm]	32.5
h_y (height of stator yoke) [mm]	12
D_{so} (stator outer diameter) [m]	325
V_t (stator teeth volume) [m^3]	1.53e-3

V_y (stator yoke volume) [m^3]	1.19e-3
σ (conductivity of silicon steel sheet) [s/m]	1694915
k_h (hysteresis loss coefficient)	179
k_e (excess loss coefficient)	3.09
k_d (lamination thickness) [mm]	0.5

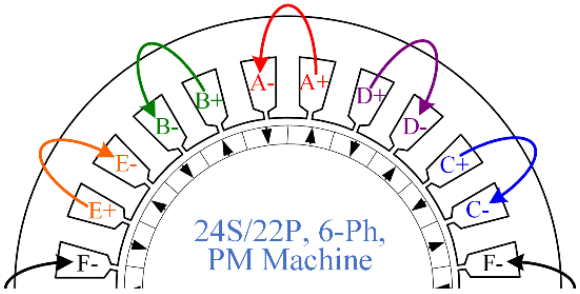

Fig. 1. 24-slot, 22-pole six-phase single-layer FSCW-PM machine (1/2 model)

The stator iron losses can be included in the objective function for loss minimization during post-fault operation. Taking the remediation method based on decoupled vector control as an example, the objective function can be modified as follows,

$$f(i_d, i_q, \lambda) = R_S(i_d^2 + i_q^2) + P_{Fe}(i_d, i_q, f) + \lambda(T^* - \psi_d(i_d, i_q) * i_q + \psi_q(i_d, i_q) * i_d)$$

(10)

where R_S is the stator resistance; T^* is the torque command; λ is the Lagrange operator.

In order to improve the accuracy, the d- and q-axis flux linkages are calculated by finite element (FE) method, as shown in Figs. 2 (a) and (b).

Combining Eqs. (6) and (7) as well as the parameters/ dimensions provided in Table I, the stator iron losses can be calculated, as illustrated in Fig. 3. As can be seen in Fig. 3, by injecting negative d-axis current, the stator iron losses can be reduced. It should be noted that the method shown in Eqs. (1)~(6) is based on the calculation of average flux density, which is not able to capture the flux density distribution around tooth pole shoe. The iron losses can be calculated by FEA as well for better accuracy. However, the material properties can be affected/ changed during steel lamination processing (punch, cut, assemble, etc.). The loss coefficients used in iron loss estimation should be adjusted based on empirical methods. The calculated losses are magnified by 1.5 times to offset this well-known effect. Surface fitting is used to obtain the functions P_{Fe} $(i_d,\ i_q)$, ψ_d $(i_d,\ i_q)$, and ψ_d $(i_d,\ i_q)$, so that the relevance can be used in post-fault control.

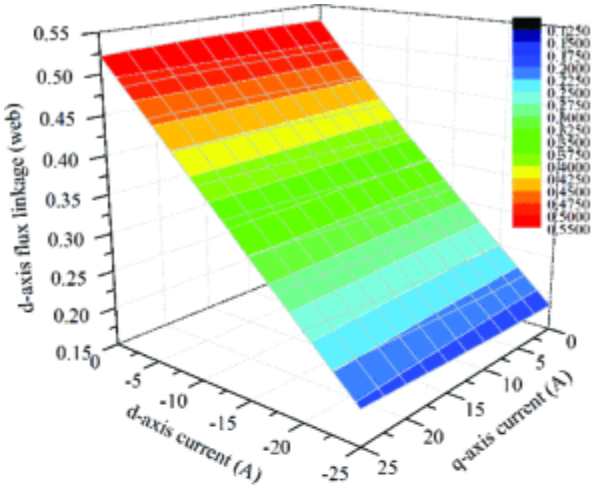

(a) d-axis flux linkage

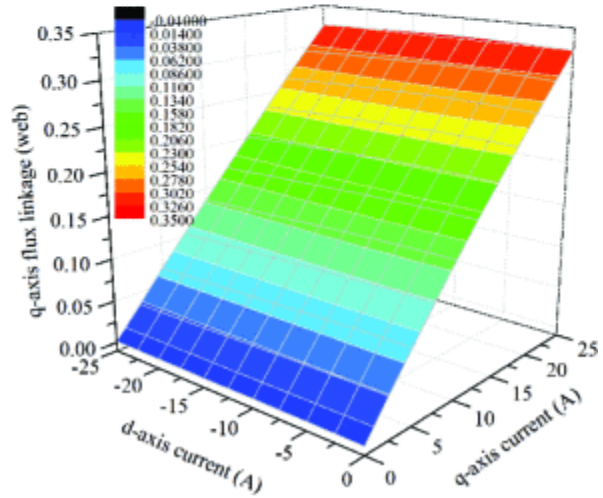

(b) q-axis flux linkage

Fig. 2. Flux linkage as a function of d- and q- axis current (d-/q- axis current: 0~25A, step: 2.5 A)

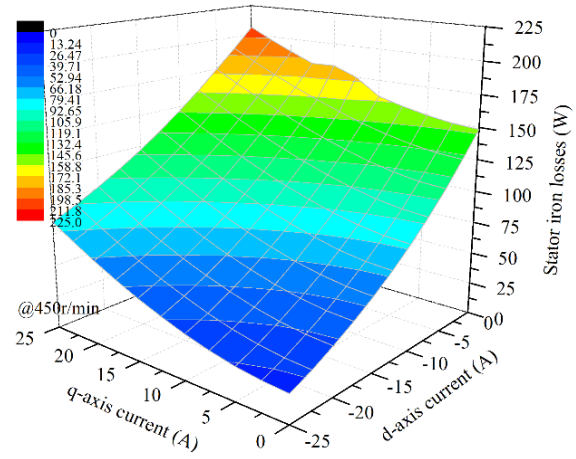

Fig. 3. Stator iron losses as a function of i_d and i_q (at 450 r/min, d-/q- axis current: 0~25A, step: 2.5 A)

C. Maximum efficiency contrl under partial load

At low-speed/high-torque region where copper losses are dominant, iron losses represent a relatively minor issue. However, at high-speed/partial-load region, iron losses can be significant. Table II shows the machine losses as well as efficiency values as a function of d- and q- axes current (q-axis current is adjusted to maintain the same electromagnetic torque) at 20% load (42.5 Nm). As can be seen in Table II, the maximum efficiency (91.7%) peaks at $i = 14.21$ A, $\gamma = 59.05°$ with the improved control method while the efficiency equals 90.3% with the conventional stator ohmic loss minimization control. This clearly implies that taking iron losses into consideration can improve machine efficiency under post-fault control.

TABLE II Machine Efficiency Calculation based on FEA (Torque command: 42.5 Nm (20% load), Speed: 450 r/min)

Post-Fault Ctrl	***Excitation***	***Losses***			***Effi.***
		Stator iron	***Copper***	***Rotor***	
Minimum P_{Fe} & P_{Cu} Ctrl	$i = 14.21$ A $\gamma = 59.05°$	80.2W	62.4W	22.5W	91.7%
Minimum P_{Cu} Ctrl	$i = 7.34$ A $\gamma = 0°$	156.9W	16.6W	20.5W	90.3%

Note: while adjusting i_d and i_q, i_{z1}, i_{z2} and i_{z3} are set to be zero.

SECTION III. Flexibility of Remediation Methods

In this section, the flexibility of post-fault remediation will be discussed based on possible combinations of three key factors /constraints. Four specific methods are selected for a detailed investigation, highlighting the influence of these constraints.

A. Key factors and constraints for post-fault control

Three key factors/constrains are selected and discussed as follows:

- *Neutral point constraint*: this refers to the constraint of the sum of all phase currents, which is determined by winding connections and inverter topologies. If star-connected winding and half-bridge voltage source converter (VSI) are adopted, the sum of all phase currents is supposed to be zero. However, this constraint can be removed through the use of open winding and full-bridge VSI (or other inverter topologies that can provide access to the neutral point, like *m*-phase (*m*+1)-leg VSI, polygonal winding connection, etc);
- *Current waveform (sinusoidal or non-sinusoidal)*: This refers to whether high-order harmonics can be injected into the winding currents. Compared to sinusoidal current waveform, non-sinusoidal current waveform generally means more harmonic components and relatively high di/dt. For a fixed pulse width modulation (PWM) switching frequency as well as DC bus voltage, high di/dt value brings challenges for the implementation of current regulation especially in the high-speed region;
- *Machine Loss Minimization*: This refers to minimization of machine copper and iron losses mentioned in Section II. Loss minimization is critical for improving machine efficiency during post-fault operation, which can determine the range of battery EV following a winding failure,

as an example. As for post-fault loss minimization, existing literature focuses on stator copper loss minimization while iron losses will be included as well in this paper.

Other than the three key factors, the maximum winding current is kept the same as rated pre-fault operation. This is because the increase of winding current amplitude will result in **(i)** higher current rating of power switches (usually means higher system cost), and **(ii)** increased thermal load (especially for FSCW machine which has features of modular design and isolation between phases). For example, in case of a two-phase open circuit failure, post-fault operation of a six-phase PM machine requires 3.46 p. u. current rating of the power switches (obtained by a method proposed in [12]). In this regard, retaining the same current amplitude for both pre- and post-fault operations is sensible for many applications. This will enable a down-rating and stable operation of a vehicle until maintenance is available.

B. Post-fault remediation methods

Based on the combination of the three key factors / constrains discussed in Section III A, four post-fault control strategies are selected for further discussions, as shown in Table III. Taking Phase-F open circuit as an example, the detailed derivation of the four post-fault remediation methods is introduced as follows. Note that the peak value of phase current is limited to 10 A_{pk}.

TABLE III Definition of Four Post-Fault Control Strategies

Remediation Method	***Neutral Point Constraint***	***Sinusoidal/Non- Sinusoidal Current***	***Machine Loss Minimization***
#1	$\sum i_j = 0$	Sinusoidal current	Not considered
#2	$\sum i_j \neq 0$	Sinusoidal current	Not considered
#3	$\sum i_j \neq 0$	Non-Sinusoidal current	Considered
#4	$\sum i_j \neq 0$	Sinusoidal current	Considered

Note: all methods maintain the same maximum value of phase winding current.

1) Remediation Method #1:

Since neutral point constraint is applied, the sum of all currents is set to be zero while the currents in the remaining five phases have the same amplitudes:

$$\sum_{j=a,b,c,d,e} i_j = 0$$

$$i_j = I_m \cos(\omega t + \theta_n) = x_n \cos(\omega t) + y_n \sin(\omega t)$$

(11)(12)

where $x_n = I_m \cos(\theta_n)$; $y_n = -I_m \sin(\theta_n)$; $n = a, b, c, d, e$.

The pre-fault synthetized stator MMF (6 phases) is,

$$F_{prefault} = 3NI_m\cos(\omega t)\cos\theta - 3NI_m\sin(\omega t)\sin\theta$$

(13)

The post-fault MMF should be equal to the pre-fault MMF,

$$\begin{cases} \sum_{j=a,b,c,d,e} Ni_j\cos(\theta_j) = -3NI_m\sin\theta \\ \sum_{j=a,b,c,d,e} Ni_j\sin(\theta_j) = 3NI_m\cos\theta \end{cases}$$

(14)

where $\theta_a = 0$; $\theta_b = -\pi/6$; $\theta_c = -\pi/2$; $\theta_d = -2\pi/3$; $\theta_e = -5\pi/6$.

By adopting Lagrange method, the minimum current required for satisfying the conditions given by Eqs. (11), (12) and (14) can be obtained. The objective function is given by,

$$L = \lambda_1\left(\sum_{j=a,b,c,d,e} i_j\right) + \lambda_2\left(\sum_{j=a,b,c,d,e} i_j\cos(\theta_j) + 3I_m\sin\theta\right)$$
$$+\lambda_3\left(\sum_{j=a,b,c,d,e} i_j\sin(\theta_j) - 3I_m\cos\theta\right) + (x_n^2 + y_n^2)$$

(15)

where λ_1, λ_2, and λ_3 are Lagrange operators. This method is generally used in a six-phase PM machine fed by a half-bridge inverter.

2) Remediation Method #2:

This method will make the minimum adjustment of winding excitation in the remaining healthy phases. This means that, in case of Phase F open circuit, the currents in Phases A, C and E will remain unchanged while the current in Phases B and D will be adjusted to form a constant rotating MMF. The current in the remaining five phases are (assume that the axis of Phase A aligns with *q*-axis when *t* = 0),

$$\begin{cases} i_a = I_m\cos(\omega t) \\ i_b = I_m\cos(\omega t - \pi/3)(shiftby - \pi/6) \\ i_c = I_m\cos(\omega t - 2\pi/3) \\ i_d = I_m\cos(\omega t - 2\pi/3)(shiftby\pi/6) \\ i_e = I_m\cos(\omega t + 2\pi/3) \end{cases}$$

(16)

Obviously, the zero-sequence current is not zero in this case.

3) Remediation Method #3:

Based on instantaneous power balance theory, mechanical power equals electrical power at any time instance,

$$T\omega = mE^T I$$

(17)

where T denotes electromagnetic torque, ω is angular speed; $m = 5$ is the number of remaining phases; E and I are winding back EMF and current vector, respectively.

Both copper and iron losses can be written as a function of stator current,

$$P_{Loss} = R_S I^T I + P_{Fe}(I)$$

(18)

where R_S is winding resistance.

The Lagrange objective function is given by,

$$L = P_{Loss}(I) + \lambda(T\omega - \sum_{j=a,b,c,d,e} e_j i_j)$$

(19)

where λ is Lagrange operator.

By solving the Lagrange equation, the expression of each phase current can be obtained. Finally, if the peak current value is higher than the rated current value, all current values will be scaled down linearly to maintain 1.0 per unit maximum phase current, i. e. $\mathrm{Max}\, I_j = I_{max}$.

4) Remediation Method #4:

The remaining five phases produce the same synthetized stator $\alpha -$ and $\beta -$axis currents as the pre-fault condition,

$$\begin{cases} i_\alpha: \sum_{j=a,b,c,d,e} i_j \cos(\theta_j) = -3I_m \sin\theta \\ i_\beta: \sum_{j=a,b,c,d,e} i_j \sin(\theta_j) = 3I_m \cos\theta \end{cases}$$

(20)

where $\theta_a = 0$; $\theta_b = -\pi/6$; $\theta_c = -\pi/2$; $\theta_d = -2\pi/3$; $\theta_e = -5\pi/6$. θ is electrical angle (d-axis: $\theta = 0$; q-axis: $\theta = \pi/2$).

The objective function is given by,

$$L = P_{Loss}(I) + \lambda_1 \left(\sum_{j=a,b,c,d,e} i_j \cos(\theta_j) + 3I_m \sin\theta \right) + \lambda_2 \left(\sum_{j=a,b,c,d,e} i_j \sin(\theta_j) - 3I_m \cos\theta \right)$$

(21)

where λ_1 and λ_2 are Lagrange operators. Again, if the peak current value is higher than the rated current value, all current values will be scaled down linearly to maintain 1.0 per unit maximum phase current.

C. Experimental results and discussions

Fig. 4 shows the test setup. The machine is fed by a full-bridge inverter comprises 24 IGBTs. In order to capture the dynamic torque, the machine is running at a relatively low speed – 150 r/min. The peak phase current amplitude is 10 A_{pk} for each test.

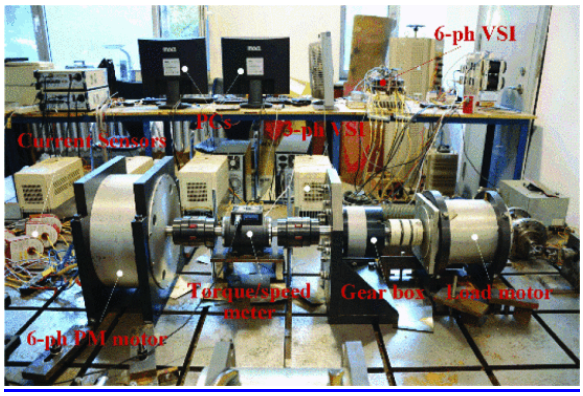

Fig. 4. Experimental setup

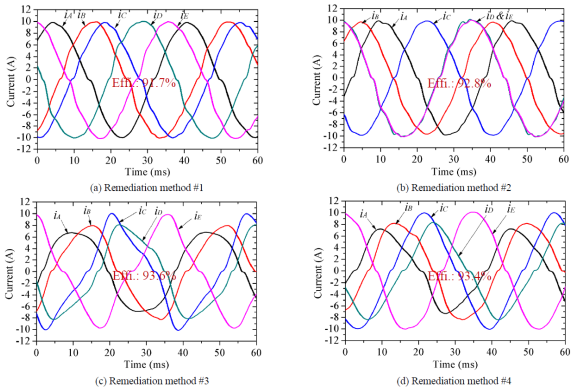

Fig. 5. Current waveforms of four remediation methods (F-phase open circuit) @ 150 r/min.

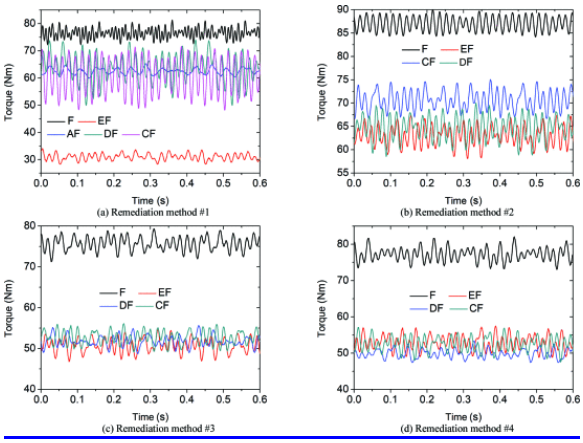

Fig. 6. Torque behavior for four remediation methods

Fig. 5 shows the current waveforms for the four remediation methods in case of Phase F open circuit while Fig. 6 shows the measured torque curves for both single- and two-phase open-circuit faults. Average torque as well as torque ripple are summarized in Tables IV and V, including the results for both single-phase and two-phase open-circuit faults. Key insights are summarized as follows,

- Electromagnetic torque reaches its maximum when the phase angles of winding current and back EMF are aligned. By adopting any fault remediation methods, the average torque is lower than faulty modes when winding current excitations in the remaining healthy phases are the same as pre-fault condition. The major benefit of post-fault control is lower torque ripple;
- Neutral point constraint (used in RM #1) generally results in higher torque ripple during post-fault operation of all faults investigated here. However, it doesn't necessarily mean lower torque performance. For some specific cases (like Phase EF open circuit), the torque capability can be fairly low (31.7 Nm) compared to other methods;
- RM #2 (the same current amplitude in all phases without neutral point constraint) shows the maximum torque capability. However, the torque per ampere and machine efficiency are low. RM #3 and RM #4 show comparable high efficiency (~93%) due to loss minimization;
- Since the tests are implemented at low speed and median torque, where copper losses dominate, it doesn't make a clear difference between copper loss minimization and the proposed comprehensive loss minimization.

TABLE IV Average Torque with Different Remediation Strategies (Current amplitude: 10A, average torque in case of normal operation (six-phase operation): 110.7N•m)

Opened phases	***F***	***EF***	***AF***	***DF***	***CF***
Faulty modes	92.9	73.5	73.5	73.5	73.5
RM #1	75.9	31.7	63.3	63.2	61.3
RM #2	86.5	63.4	--	68.4	63.4
RM #3	78.9	53.7	--	55.2	53.8
RM #4	79.0	54.4	--	55.0	54.9

Note: angle between Phases A and F is 90 deg. For open-winding/full-bridge topology (used in RM #2~#4), post-fault control is not required.

TABLE V Torque Ripple with Different Remediation Strategies (Unit: %; Normal: ΔT/Tav=4.1%)

Opened phases	***F***	***EF***	***AF***	***DF***	***CF***
Faulty modes	19.7	22.4	5.0	17.0	21.1
RM #1	12.1	20.1	8.5	40.1	39.3
RM #2	6.8	16.1	--	12.1	18.1
RM #3	10.9	15.2	--	13.7	15.0
RM #4	11.7	16.4	--	12.2	18.1

In order to better understand the differences between the four remediation methods, current excitations are transferred into "$dqz_1z_2z_3$" plane through Eqs. (2) and (3), as shown in Fig. 7. The ideal excitations derived in Section III B are used instead of the testing results.

Key insights from Fig. 7 include the following:

- Although the average value of d-axis current is almost zero, there are dynamic d-axis current fluctuations from 1.5 A to -1.5 A for all the four remediation methods;
- The q-axis current trajectories of the four methods are ellipses rather than perfect circles. The minor axes are all aligned with the axis of Phase F. The area of the current ellipses represents the torque-producing capabilities. Under the 1.0 per unit current constraint, RM #2 produces the maximum torque while RM #1 gives the minimum torque;
- The reason why d- and q-axis current values are not constant is that all remediation methods are based on a perspective of a pre-fault six-phase system rather than a five-phase unbalanced system;
- As can be seen from Figs. 7 (c)~(e), for RM #3 and RM #4 zero-sequence currents are always with zero values. However, for RM #1 and RM #2, there are significant zero-sequence currents which don't produce any torque but generate more losses.

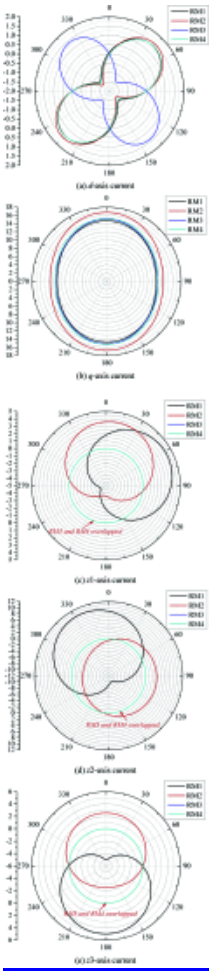

Fig. 7. *d*-*q*-*z*1-*z*2-*z*3 currents in polar coordinate plane for remediation methods #1~#4 in case of phase F open circuit (the current references are used instead of the measured currents)

SECTION IV. Conclusions

This paper investigates maximum efficiency control following winding open circuit faults. The iron losses estimation is based on numerical analysis of flux linage and closed-form calculation of iron losses. The results show that the efficiency can be boosted compared to the existing post-fault control in which only the stator ohmic losses are considered for loss minimization.

Three key factors/constraints have been discussed defining the post-fault control. Four post-fault control strategies have been compared in terms of machine key performance parameters including average torque, torque ripple and efficiency. It has been found that under 1.0 per unit current constraint, Remediation Method #2 can produce the maximum torque while Remediation Method #3 and #4 generate the minimum losses and preserve energy. The results of Remediation Method #1 show that the neutral point constraint limit the torque-producing capability and machine efficiency, but minimum switch counts are required for post-fault control. The flexibility of post-fault control in the six-phase PM machine can be leveraged for different operating points where either high output torque or high efficiency are required.

ACKNOWLEDGMENT

The author would like to thank ANSYS for making their Maxwell finite element software available for use in this investigation.

References

1. E. Levi, "Advances in converter control and innovative exploitation of additional degrees of freedom for
2. L. Parsa and H. Toliyat, "Five-phase permanent-magnet motor drives", *IEEE Trans. Ind. Appl.*, vol. 41, no. 1, pp. 30-37, Jan./Feb. 2005.
3. S. Dwari and L. Parsa, "Fault-tolerant control of five-phase permanent-magnet motors with trapezoidal back EMF", *IEEE Trans. Ind. Electron.*, vol. 58, no. 2, pp. 476-485, Feb. 2011.
4. A. Mohammadpour and L. Parsa, "Global fault-tolerant control technique for multiphase permanent-magnet machines", *IEEE Trans. Ind. Appl.*, vol. 51, no. 1, pp. 178-186, Jan./Feb. 2015.
5. N. Bianchi, S. Bolognani and M. D. Pre, "Impact of stator winding of a five-phase permanent-magnet motor on postfault operations", *IEEE Trans. Ind. Electron.*, vol. 55, no. 5, pp. 1978-1987, May 2008.
6. F. Wu, C. Tong, Y. Sui, L. Cheng and P. Zheng, "Influence of third harmonic back EMF on modeling and remediation of winding short circuit in a multiphase PM machine with FSCWs", *IEEE Trans. Ind. Electron.*, vol. 63, no. 10, pp. 6031-6041, Oct. 2016.
7. A. M. EL-Refaie, T. M. Jahns, P. B. Reddy and J. W. McKeever, "Modified vector control algorithm for increasing partial-load efficiency of fractional-slot concentrated-winding surface PM machines", *IEEE. Trans. Ind. Appl.*, vol. 44, no. 5, pp. 1543-1551, Sept./Oct. 2008.
8. R. Ni, D. Xu, G. Wang, L. Ding, G. Zhang and L. Qu, "Maximum efficiency per ampere control of permanent-magnet synchronous machines", *IEEE Trans. Ind. Electron.*, vol. 62, no. 4, pp. 2135-2143, Apr. 2015.
9. Y. Zhao and T. A. Lipo, "Modeling and control of a multi-phase induction machine with structural unbalance", *IEEE Trans. Energy Convers.*, vol. 11, no. 3, pp. 570-577, Sept. 1996.
10. R. Kianinezhad, B. Nahid-Mobarakeh, L. Baghli, F. Betin and G.-A. Capolino, "Modeling and control of six-phase symmetrical induction machine under fault condition due to open phases", *IEEE Trans. Ind. Electron.*, vol. 55, no. 5, pp. 1966-1977, May 2008.
11. G. Bertotti, "General properties of power losses in soft ferromagnetic materials", *IEEE Trans. Magn.*, vol. 24, no. 1, pp. 621-630, 1988.
12. F. Baudart, B. Dehez, E. Matagne, D. Telteu-Nedelcu, P. Alexandre and F. Labrique, "Torque control strategy of polyphase permanent-magnet synchronous machines with minimal controller reconfiguration under open-circuit fault of one phase", *IEEE Trans. Ind. Electron.*, vol. 59, no. 6, pp. 2632-2644, June 2011.